*Highlights of Spanish Astrophysics VI, Proceedings of the IX Scientific Meeting of the Spanish Astronomical Society held on September 13 - 17, 2010, in Madrid, Spain. M. R. Zapatero Osorio et al. (eds.)*

# Evolutionary state of the Ly$\alpha$ emitter Haro 2

**H. Otí-Floranes[1,2] and J. M. Mas-Hesse[1]**

[1] Centro de Astrobiología – Departamento de Astrofísica (INTA–CSIC), POB 78, 28691 Villanueva de la Cañada, Spain. otih@cab.inta-csic.es, mm@cab.inta-csic.es
[2] Dpto. de Física Moderna, Facultad de Ciencias, Universidad de Cantabria, 39005 Santander, Spain

## Abstract

We present the study of the star formation activity in Haro 2, a Ly$\alpha$ emitter, blue compact galaxy in the Local Universe. Given the similarities of Haro 2 with more distant galaxies, we aim to understand the Ly$\alpha$ emission in a local prototype in order to better interprete this emission in star-forming galaxies at high redshifts. Starbursting activity inside the galaxy releases huge amounts of mechanical energy. As a consequence the surrounding gas is accelerated and heated, producing intense soft X-ray radiation. Moreover, the outflow of the neutral gas might allow the escape of Ly$\alpha$ photons emitted by recombination. We believe that the turbulent motion of the gas generates an additional component of diffuse collisional Ly$\alpha$ emission, which we find to coincide spatially with the soft X-ray emission, and not with the Balmer lines produced by recombination. A correct understanding of these processes is essential to properly calibrate the star formation rate in high-redshift galaxies as a function of the Ly$\alpha$ intensity.

## 1 Introduction

Starbursts are conspicuous sources of ionizing photons which can interact with the surrounding gas and produce nebular emission lines by recombination processes. Although simple nebular models predict Ly$\alpha$ to be $\sim 9$ times more intense than the conspicuous H$\alpha$ line, observations show that its presence, intensity, spectral shape and spatial profile do depend on many factors [19]. Ly$\alpha$ is a resonant line and this causes Ly$\alpha$ photons to be absorbed and reemited by hydrogen atoms within the nebular gas many times before they can escape, and very little dust can completely extinguish the line. However Ly$\alpha$ can escape when the mechanical energy injected by starbursts into the interstellar medium (ISM) causes the neutral gas to outflow, by shifting the absorption to bluer wavelengths [18]. At the same time, this outward-push heats the gas surrounding the clusters up to temperatures of millions of Kelvin, hence leading to X-ray emission.

Table 1: Haro 2 coordinates, distance, scale, galactic columnn density [9] and color excess towards the source and oxygen abundance [4].

| R. A. (J2000.0) | Decl. (J2000.0) | Distance (Mpc) | Scale (pc arcsec$^{-1}$) | $N$(HI) (cm$^{-2}$) | $E(B–V)_{\rm Gal}$ | $12+\log$(O/H) |
|---|---|---|---|---|---|---|
| 10 32 31.9 | +54 24 03.7 | 20.5 | 100 | $6.3\times10^{19}$ | 0.012 | 8.5 |

Haro 2 is a local dwarf galaxy with conspicuous star formation [10] causing soft X-ray emission [15] and which, despite being a metal-rich blue compact dwarf galaxy ($Z = Z_{\odot}/2$ [4]) does show a prominent Ly$\alpha$ emission with a P-Cygni profile, apparently produced by a superbubble of neutral gas expanding at 200 km s$^{-1}$ [9]. The bolometric luminosity of Haro 2 overlaps with the low-end of $L_{\rm FIR}$ in Lyman Alpha Emitting Galaxies at $z = 3.1$ [5, 6] and it also shows a UV emission similar to the weakest Lyman Break Galaxies in the redshift range $z = 2.7$–5 [17]. This fact, together with its high Ly$\alpha$-intensity and P-Cygni spectral profile, makes of Haro 2 a good local prototype of high-$z$ Ly$\alpha$-emitters. Given that the Ly$\alpha$ line is generally the only tool available for quantifying the star formation activity in distant galaxies, Haro 2 can lead us to a better understanding of Ly$\alpha$ emission in those sources and thus of the cosmological evolution of star formation.

In this paper we use optical, UV and X-ray spectral-imaging data from HST and *Chandra* to describe the present starburst episode in Haro 2 and the effects of this star formation activity on the soft X-ray and Ly$\alpha$ radiation detected. Coordinates and basic data of Haro 2 are listed in Table 1.

## 2 Analysis and results

As shown in the FOC image of Fig. 1 the elliptically-shaped nucleus of Haro 2 hosts two star-forming regions, which we identify as knot SE and knot NW. Both knots are aligned in the northwest direction separated by $\sim$ 75–100 pc, and while knot SE is not resolved, knot NW is more extended, which confirms its more complex morphology. UV radiation extends a few hundreds of parsecs away from the knots, which should be considered as the star-bursting region with a size of $\sim 750\times1000$ pc$^2$. UV-flux value for each knot and for the whole starburst region was extracted from the FOC image considering boxes with sizes $7.4''\times5.5''$ for knot NW and $7.4''\times4.8''$ for knot SE. Due to the proximity between knots NW and SE the origin of the counts could not be discerned unambiguously, hence the total flux of the whole nucleus $F_{2328}= 2.7\times10^{-14}$ erg s$^{-1}$ Å$^{-1}$ cm$^{-2}$ should be taken as a more reliable measure. $F_{2328}$ values for each knot together with their sizes are listed in Table 2.

Normalized spectra for both stellar knots in the wavelength range 1200–1700 Å were extracted from the STIS spectral image obtained in direction D2 with filter G140L, considering a spatial extension for the stellar continuum regions of $0.6''$ and $1.5''$ for knots SE and

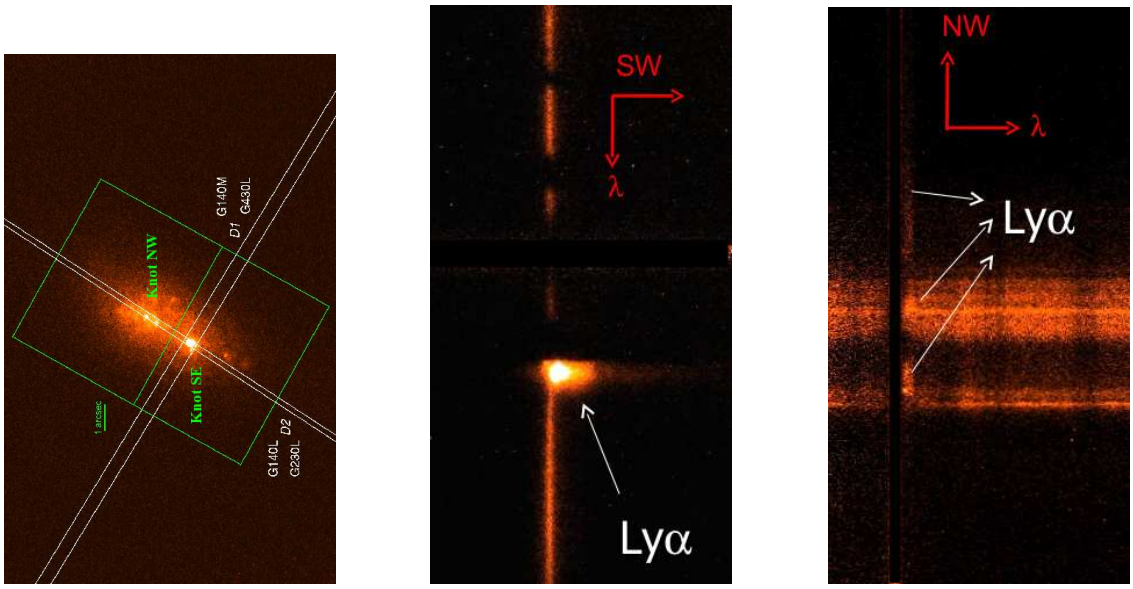


Figure 1: Ultraviolet image of HST/FOC of Haro 2 (left), together with the positions of the slits in the observations of HST/STIS D1 with G140M and G430L [11], and D2 with G140L and G230L [3], and the boxes used to extract the UV flux from each knot. North is up and east is left. Spectral images of Haro 2 obtained with HST/STIS G140M (center) and G140L (right) taken along directions D1 and D2, respectively.

NW, respectively. High spectral resolution synthetic UV spectra were obtained from Starburst99 models [8] (hereinafter SB99 models) in the range 1200–1800 Å, assuming a Salpeter Initial Mass Function, instantaneous star formation and a metallicity $Z = 0.008$. Fitting of the normalized spectral profiles of the stellar absorption lines Si IV1394, 1403 and C IV1548, 1551 yielded ages $\sim 4$ Myr for knot SE and $\sim 5$ Myr for knot NW, which are in agreement with results in the literature [10, 3]. In order to calculate the reddening, the SEDs of the knots were fitted with the SEDs provided by the SB99 models for the best fitting parameters, obtaining $E(B–V)_{\rm knot\,SE} \sim 0.050$ and $E(B–V)_{\rm knot\,NW} \sim 0.020$ when assuming the SMC extinction law [13]. Finally, masses of the knots were calculated dividing the observed UV fluxes integrated on the FOC image over the extension of each knot by the values predicted by SB99.

Spectral images on the ultraviolet along the minor (D1 direction) and major (D2 direction) axis in the Ly$\alpha$ wavelength range are displayed in Fig. 1. Spatial profiles of the Ly$\alpha$ emission, UV continuum and H$\alpha$ emission are shown on the left panel of Fig. 2. Knot SE shows a Ly$\alpha$ emission $\sim 600$ pc large, detached from the stellar continuum, and which is formed by one strong, compact component close to the stellar emission, which extends over $\sim 250$ pc, and another weaker and more diffuse emission extending to $\sim 350$ pc in the southwest direction. On the other hand, the Ly$\alpha$ emission seems to be more complex along the D2 direction with regions of total absorption and others showing clear emission. While the stellar continuum shows two clear peaks associated to the stellar knots, the Ly$\alpha$-profile is found in

Table 2: Physical properties of knots NW and SE in Haro 2. Luminosity values are corrected for the intrinsic absorption calculated assuming [13] as well as for Galactic absorption. Extension of stellar continuum along direction D2 in STIS spectral image is shown.

| Knot | Age (Myr) | Mass ($M_\odot$) | $E(B–V)$ | $F_{2328}$ (erg s$^{-1}$ Å$^{-1}$ cm$^{-2}$) | $L_{2328}$ (erg s$^{-1}$ Å$^{-1}$) | Extension (pc) |
|---|---|---|---|---|---|---|
| Knot SE | $\sim 4$ | $7.0 \times 10^5$ | 0.050 | $1.1 \times 10^{-14}$ | $3.5 \times 10^{38}$ | $\sim 60$ |
| Knot NW | $\sim 5$ | $1.3 \times 10^6$ | 0.020 | $1.7 \times 10^{-14}$ | $6.5 \times 10^{38}$ | $\sim 150$ |

emission in three different regions: 1) northwest of knot NW, totally detached from the stellar continuum and extending over $\geq 600$ pc (emission Ly$\alpha_{\rm NW\,A}$, $F$(Ly$\alpha$) $= 1.8 \times 10^{-14}$ erg s$^{-1}$ cm$^{-2}$ not corrected for any kind of absorption), 2) within knot NW, over $< 50$ pc (emission Ly$\alpha_{\rm NW\,B}$, $F$(Ly$\alpha$) $= 5 \times 10^{-15}$ erg s$^{-1}$ cm$^{-2}$), and 3) northwest from knot SE and $\sim 100$ pc long (emission Ly$\alpha_{\rm SE\,2}$, $F$(Ly$\alpha$) $= 1.6 \times 10^{-14}$ erg s$^{-1}$ cm$^{-2}$). While Ly$\alpha_{\rm NW\,A}$ is very diffuse and extended, the Ly$\alpha_{\rm SE\,2}$ and Ly$\alpha_{\rm NW\,B}$ contributions seem to be rather more compact. However, the diffuse emission Ly$\alpha_{\rm NW\,A}$, although dimmer than the other two components, is the strongest one when integrated over its full extension. A similar effect has been also found in Haro 11 [7], another strong Ly$\alpha$ emitter, star-forming galaxy in the Local Universe. On the other hand, emissions Ly$\alpha_{\rm SE\,2}$ and Ly$\alpha_{\rm NW\,B}$ seem to be produced by recombination in gas surrounding the clusters given their overlap with the H$\alpha$-emitting regions. The fact that these Ly$\alpha$ photons are able to escape from these regions indicates that the neutral hydrogen surrounding them either has a very low column density, or is outflowing with a significant velocity, as already derived from the P Cygni profile shown in the high resolution spectra around knot SE.

In the 3-color X-rays image of Haro 2 shown in Fig. 2 an extended, diffuse soft emission is detected associated to the gas being heated by the supernovae and stellar winds originated in the central starbursts, as well as a hard emission from a point-like source located in knot SE. X-ray spectral fitting yielded a model with a hot plasma emission (HP, hereinafter) plus a power-law component (PL, in what follows) attenuated by both intrinsic and Galactic absorptions ($N$(HI)$_{\rm int} = 7.0 \times 10^{19}$ cm$^{-2}$, $N$(HI)$_{\rm Gal} = 6.3 \times 10^{19}$ cm$^{-2}$). Main contributors to the X-ray energy range 2–15 keV in starburst galaxies are accreting neutron stars or black holes [12], and given the intense, hard emission observed we assumed that a high mass X-ray binary (HMXB) is located in knot SE. We assumed the typical range $\Gamma = 1.0$, 1.2 found for the PL photon index in HMXBs [20, 14], which satisfactorily reproduced the small contribution of PL to the soft X-ray band we had derived from the fits. The value we obtained in our study for $kT \sim 0.73^{+0.09}_{-0.10}$ keV is similar to the values found in other star-forming galaxies [16, 7]. Given the soft X-ray luminosity value $L_{0.4-2.4\,\rm keV} \sim 2.3^{+0.5}_{-0.5} \times 10^{39}$ erg s$^{-1}$ yielded by our analysis and the properties found for knots SE and NW, CMHK02 evolutionary synthesis models [2] predict a value for the efficiency in the conversion of mechanical energy injected by the bursts into X-ray luminosity of 2–3 %, which agrees with the value of 2 % found by [15]. On the other hand, the high hard X-ray luminosity found $L_{2.0-10.0\,\rm keV} \sim 2.4^{+1.4}_{-1.4} \times 10^{39}$ erg s$^{-1}$ indicates that the hard source located in knot SE might indeed be an ULX candidate.

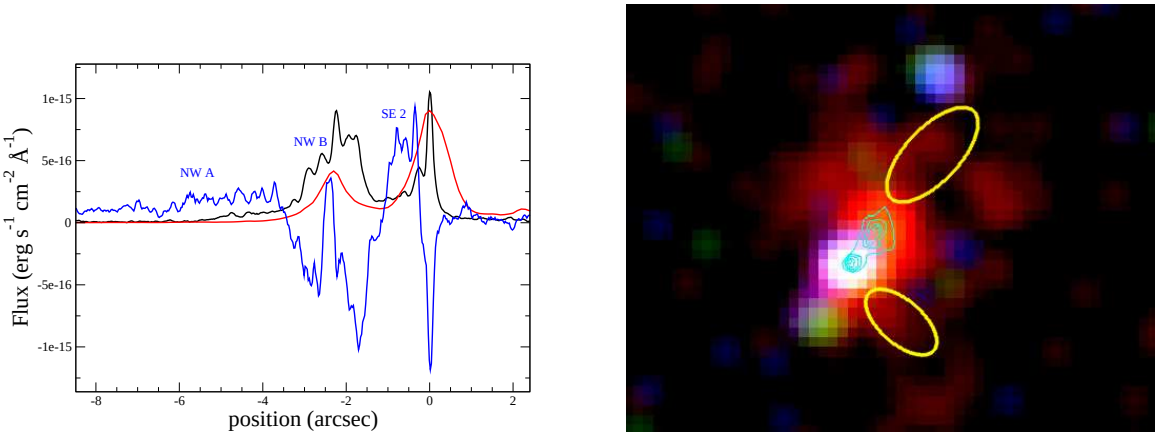


Figure 2: *Left*: Emission profile of Ly$\alpha$ (blue), UV continuum from STIS data (2330 Å, black) and H$\alpha$ profile from WFPC2 data (red) along direction D2. Units are valid for Ly$\alpha$ whereas for the other magnitudes intensity is relative. *Right*: Chandra colour X-ray image of Haro 2, with soft (0.2–1.5 keV, red), medium (1.5–2.5 keV, green) and hard (2.5–8.0 keV, blue) emissions, together with the HST/NICMOS contours of the near-infrared. Regions whithin the yellow ellipses show diffuse Ly$\alpha$ emission. North is up and east is left.

The origin of the diffuse Ly$\alpha$ emission is unclear, since it is not correlated with the H$\alpha$ emission produced by recombination. Ly$\alpha$ emission might originate from recombination processes and/or collisional excitations, being proportional to coefficient $\alpha^{\rm eff}_{{\rm Ly}\alpha}$ and $q^{\rm eff}_{{\rm Ly}\alpha}$, respectively. $q^{\rm eff}_{{\rm Ly}\alpha}$ is of the same order of magnitude as $\alpha^{\rm eff}_{{\rm Ly}\alpha}$ for electronic temperatures $\sim 10^4$ K, but it becomes two orders of magnitude greater at $\sim 2\times10^4$ K and even greater at higher temperatures [1]. Therefore, as long as there is a sufficient number of neutral hydrogen atoms, the collisional contribution can exceed the recombination componet in environments with high temperature. We argue that the diffuse Ly$\alpha$ emission observed in knot NW extending more than 600 pc in the D2 direction (Ly$\alpha_{\rm NW\,A}$) and the weak, diffuse emission in knot SE observed along D1 direction might be of collisional nature, given the utter absence of stellar and H$\alpha$ emissions in the regions they are found in, and due to their large extension and dim intensity. As we observe in Fig. 2 these Ly$\alpha$ diffuse components coincide spatially with diffuse, soft X-ray emission originated by the heating of the interstellar gas surrounding the stellar clusters by mechanical energy injected into the ISM during the starburst life through stellar winds and supernovae. This environment could provide the different phases needed for collisional contribution of the line to be produced: hot gas to increase the collisional emission and neutral atoms with bound electrons to be excited by the energetic free electrons from this hot gas. The fact that the nebular collisional radiation producing Ly$\alpha$ diffuse emission and the soft X-ray emission might have the same physical origin as an interaction of gases with different temperatures reinforces the idea that the diffuse Ly$\alpha$ emission observed could be due to collisional excitation of neutral atoms by the hot gas, instead of being produced by recombination. Nevertheless, our data do not allow to reject other models, which assume

that the diffuse Ly$\alpha$ emission might be associated to Ly$\alpha$ photons leaking from the neutral gas after multiple, resonant scattering [7].

## Acknowledgments

JMMH and HOF are partially funded by Spanish MICINN grants CSD2006-00070 (CONSOLIDER GTC), AYA 2007-67965 and AYA2008-03467/ESP. HOF is funded by Spanish FPI grant BES-2006-13489. We thank Elena Jiménez Bailón and Giovanni Miniutti for their help in the X-ray analysis.

## References

[1] Cantalupo, S., Porciani, C., & Lilly, S. J. 2008, ApJ, 672, 48

[2] Cerviño, M., Mas-Hesse, J. M., & Kunth, D. 2002, A&A, 392, 19

[3] Chandar, R., Leitherer, C., & Tremonty, C. A. 2004, ApJ, 604, 153

[4] Davidge, T. J. 1989, PASP, 101, 494

[5] Gawiser, E., et al. 2007, ApJ, 671, 278

[6] Gronwall, C., et al. 2007, ApJ, 667, 79

[7] Hayes, M., et al. 2007, MNRAS, 382, 1465

[8] Leitherer, C., et al. 1999, ApJS, 123, 3

[9] Lequeux, J., Kunth, D., Mas-Hesse, J. M., & Sargent, W. L. W. 1995, A&A, 301, 18

[10] Mas-Hesse, J. M., & Kunth, D. 1999, A&A, 349, 765

[11] Mas-Hesse, J. M., Kunth, D., Tenorio-Tagle, G., Leitherer, C., Terlevich, R. J., & Terlevich, E. 2003, ApJ, 598, 858

[12] Persic, M., & Rephaeli, Y. 2002, A&A, 382, 843

[13] Prévot, M. L., et al. 1984, A&A, 132, 389

[14] Shaw Greeening, L., et al. 2009, A&A, 495, 733

[15] Summers, L. K., Stevens, I. R., & Strickland, D. K. 2001, MNRAS, 327, 385

[16] Summers, L. K., Stevens, I. R., Strickland, D. K., & Heckman, T. M. 2004, MNRAS, 351, 1

[17] Tapken, C., et al. 2007, A&A, 467, 63

[18] Tenorio-Tagle, G., et al. 1999, MNRAS, 309, 332

[19] Verhamme, A., Schaerer, D., & Maselli, A. 2006, A&A, 460, 397

[20] White, N. E., Swank, J. H., & Holt, S. S. 1983, ApJ, 270, 711